Journal of Colloid and Interface Science 332 (2009) 165–172

Contents lists available at ScienceDirect

Journal of Colloid and Interface Science

www.elsevier.com/locate/jcis

Preparation of honeycomb scaffold with hierarchical porous structures by core-crosslinked core–corona nanoparticles

Xiang Yao [a], Hongwei Yao [b,*], Yuanting Li [a], Gang Chen [b]

[a] Department of Chemical Engineering, Tsinghua University, Beijing 100084, People's Republic of China
[b] Department of Polymer Science and Engineering, Qingdao University, Qingdao 266071, People's Republic of China

ARTICLE INFO

Article history:
Received 13 August 2008
Accepted 4 December 2008
Available online 10 December 2008

Keywords:
Emulsion template
Honeycomb scaffold
Core–corona nanoparticles
Amphiphilic block copolymer

ABSTRACT

The preparation of honeycomb scaffold with hierarchical controllable porous structures is reported. The ABA three block amphiphilic copolymer PS-b-P(St-Alt-AMn)-b-PS was synthesized through reversible addition fragmentation chain transfer polymerization (RAFT) and subsequently self-assembled to core–corona nanoparticles with the middle block P(St-Alt-AMn) as the core and two side block PS as the corona. The formed core–corona nanoparticles were further crosslinked through the reaction of amino diphenyl methane with anhydride in chains. The core-crosslinked core–corona nanoparticles were used as the building block to fabricate the controllable porous scaffold with hierarchical structure. The micrometer level honeycomb mesostructures can be obtained by an inverse emulsion template method which is consisted in the formation of the high internal phase ratio emulsions (HIPRE) while the nanometer level pores are formed by the close-packed core–corona block copolymer nanoparticles. As carboxylic group is formed in the crosslink step of the core, the growth factor can be easily incorporated into the matrix in order for the growth of the cell in the tissue engineering application. This kind of hierarchical honeycomb structure is an ideal candidate for the tissue engineering and drug delivery applications.

1. Introduction

In recent years, the control of three-dimensional structures in nanometer or micrometer scales has drawn a lot of attention for its potential applications such as tissue engineering [1–4], separation, microreactors, biointerfaces [5,6], catalysts, microstructured electrode surfaces [7], and photonic band gap crystals [8]. In the application of tissue engineering or other biomimetic fields, a sort of porous scaffold with hierarchically multilevel length of pores is desirable [1,2]. First, micrometer scale pores are required to facilitate the cell to migrate in. Second, controllable nanoscale structures are also necessary. The vivo environment of cells is a three-dimensional complex extracellular matrix (ECM) with various nanoscale fibers and pores. To simulate this true biological environment, a similar stereotype structure is needed [9]. Although the natural materials such as the collagen have the desired structures described above, it is hard to control the structure of the collagen itself. Thus it is necessary to fabricate the scaffold using a kind of building blocks with nanoscale controllable structures. That is to say, fabricating tissue engineering scaffold demands hierarchically controllable structure. Unfortunately, most of the methods used to prepare the scaffolds can only fit one of the dual level control. For instance, the salt leaching [10], phase inversion [11] and freeze-drying [12] methods can only produce porous scaffolds with the pore size of micrometer scale. Nanometer scale pores can be obtained by the electro-spun [13,14] technique, however, the macropores which is required for the entrance of the cell to the tissue matrix is hard to be produced by this method. Recently, Stratford et al. [15] have predicted the possibility of making the bicontinuous three-dimensional (3D) structure by the jammed colloidal spheres in computer simulation. This kind of 3D structure has the merit of dual scale controllable structures described above, in which the micrometer scale bicontinuous structure can be tuned by liquid–liquid phase separation, while the colloids can be jammed and fixed into one phase of the liquids to form the matrix. The space between the colloidal spheres and the structure of the colloid themselves are both tunable under nanometer scale. This kind of hierarchically porous structure is an ideal mode for the tissue engineering scaffold fabrication.

As firstly reported by Francois et al. [16], the emulsion template method offered an opportunity to prepare mesoporous honeycomb membrane. This kind of porous membrane can be obtained by exposing the polymer/carbon disulfide solution to a flow of moist air. Either the monolayer or multilayer porous structure can be obtained by adjusting the polymer molecular architecture, polymer

* Corresponding author. Fax: +86 0532 85952540.
E-mail address: yaohwqd@qdu.edu.cn (H. Yao).

0021-9797/$ – see front matter
doi:10.1016/j.jcis.2008.12.015

concentration and polymer molecular weight, etc. As reviewed by Rodríguez-Abreu et al. [17], this method is essentially based upon the formation of HIPRE [18]. Emulsions are usually two immiscible liquids with one liquid (internal phase) dispersed in another (the continuous or external phase). Especially HIPRE is a sort of concentrated emulsions possessing a large volume of internal phase (the volume fraction is above 0.74). The high volume fraction of internal phase results in the internal phase droplets deformed into honeycomb patterns, which are separated by continuous phase of thin films. In the case of HIPRE emulsion template, diverse block copolymers, often polystyrene-based, can be used to form the external phase and the condensed water droplets to form the internal phase. The evaporation of the solvent induces the phase separation of the polymer to lock the structure of the external phase and thus form the film matrix.

On the other hand, the core–corona nanoparticles formed by the self-assembly of the amphiphilic copolymers are useful building block for many applications. As reviewed by Wooley et al. [19], the idea of crosslinkable core–corona structure is inspired from biology, which characterizes a structure constructed by the weak electrostatic interaction and further stabilized by the strong chemical bond. The core–corona nanoparticle not only has the similar structure with biological organism but also has a more controllable functional parts compared with the common colloids. Both the core and corona can be crosslinked to form a more compact nanoparticle. The corona usually can be tailored to be sensitive to the environment and the core can be functionalized to make the drug delivery possible. With the recent development of the controlled radical living polymerization such as atom transfer radical polymerization (ATRP) and RAFT, the core–corona nanoparticles can be more easily prepared [20]. This kind of biology inspired structure is an ideal building block which can be used for the fabrication of the hierarchically multilevel porous tissue engineering scaffold.

In this work, we synthesized an ABA type three block amphiphilic copolymer polystyrene-b-poly(styrene-alt-maleic anhydride)-b-polystyrene, abbreviated as PS-b-P(St-alt-MAn)-b-PS, using RAFT polymerization. The core–corona nanoparticles are fabricated through the self-assembly of the amphiphilic block copolymer in xylene with the corona formed by the PS side block and core formed by the maleic anhydride middle block. The middle block core is crosslinked through the reaction of amino diphenyl methane with anhydride in chains and the obtained carboxylic groups enable the growth factor agents incorporated for the tissue engineering applications. The obtained core-crosslinked core–corona nanoparticles are used to form the mesoporous honeycomb membrane using the inverse emulsion template method described above. This kind of mesoporous membrane has hierarchical structure with two-level scale controllable, namely mesoscale and nanoscale. It experimentally demonstrated the simulation work done by Stratford et al. [15] and is an ideal mode for the scaffold fabrication for the tissue engineering applications.

2. Materials and methods

2.1. Materials

All solvents were dried using standard procedures. Styrene (St) (AR grade, the development center of Tianjing Komiou Chemical Agent) was washed with 10% NaOH and de-ionized water, and dried, then distilled from calcium hydride immediately prior to use. 2,2-Azobis(isobutyronitrile) (AIBN) was recrystallized from ethanol. Maleic anhydride (Man) (AR grade, Beijing Yili Chemical Agent Co.), carbon bisulfide (CS_2), tetrahydrofuran (THF) (AR grade, Shanghai Sihaowei Chemical Engineering Co.), amino diphenyl methane (Shanghai Senni Chemical Engineering Co.) were used without further purification. Dibenzyl trithiocarbonate (DBTTC), synthesized according to literature [21].

2.2. RAFT polymerization of PS macro-CTA

The RAFT polymerization of PS was conducted in a sealed ampule. DBTTC (0.58 g, 2 mmol), St (24 g, 0.23 mol) and AIBN (0.016 g, 0.1 mmol) were charged into the glass ampule containing 20 g toluene. The mixture was degassed through three freeze–thaw cycles. The ampule was then sealed under vacuum and kept in an oil bath at 90 °C to conduct the polymerization. After 5 h, the ampule was put into liquid nitrogen to stop the polymerization. The mixture was precipitated in *N*-hexane of 15 times excess. This precipitation procedure was repeated three times and dried under vacuum. The resulted yellow powder was PS and stored to be used as the macro-chain transfer agent (macro-CTA).

2.3. Synthesis of PS-b-P(St-alt-MAn)-b-PS

The RAFT polymerization of PS-b-P(St-alt-MAn)-b-PS was conducted in a sealed ampule. In a typical run, St (10.4 g, 0.1 mol), MAn (9.8 g, 0.1 mol) and AIBN (40 mg) were charged into the glass ampule containing 20 g THF together with 6.75 g PS macro-CTA. The mixture was degassed through three freeze–thaw cycles. The ampule was then sealed under vacuum and kept in an oil bath at 60 °C to conduct the polymerization. After 20 h, the mixture was precipitated in *N*-hexane of 15 times excess. This precipitation procedure was repeated three times and dried under vacuum. The resulted yellow powder was PS-b-P(St-alt-MAn)-b-PS. The number of the repeat units of respective blocks was calculated from the NMR data. To determine the anhydride content within the obtained three block copolymer, PS-b-P(St-alt-MAn)-b-PS (1.5 g) was dissolved into 40 ml butanone. After the sample was dissolved, 6 ml pyridine and 6 ml water were added under stirring. The stirring was continued for another 4 h and then the sample was titrated by KOH–ethanol solution using Thymol blue (1%) as the indicator. ^{1}H NMR ($CDCl_3$ 600 MHz): δ 0.8607 (m, 1H), 1.2624 (m, 2H), 1.7598 (m, 1H), 2.5027 (t, 1H), 2.5905 (m, 1H).

2.4. General procedures for core-crosslinked self-assembly

The block copolymers obtained above (1 g) were dissolved in 5 ml of THF respectively. Toluene was then added dropwise under stirring through a syringe at a rate of 1 drop every 5 s. At desired toluene/THF ratio, toluene addition was stopped, and the mixture was kept stirring for an additional 12 h. According to the anhydride content, amino diphenyl methane dissolved in THF (1 g/100 ml) was then added to the above mixture as the crosslink reagent to form the core crosslinked core–corona nanoparticles.

2.5. Preparation of honeycomb film

The nanoparticles obtained above were dissolved in CS_2 with concentration from 0.5 to 5%. The solution of the nanoparticles is coated onto a glass slide, moist airflow was introduced above the solution at the rate of 20 cm/s, the humidity was controlled above 80%. The solvent evaporated in about 6 s and the solution on the glass slide became a turbid translucent film. The film took on different colors seen from different angles.

2.6. Characterization

2.6.1. Nuclear magnetic resonance (NMR) spectroscopy

All ^{1}H NMR spectra were recorded using a Bruker 600 MHz spectrometer. Samples were analyzed in $CDCl_3$.

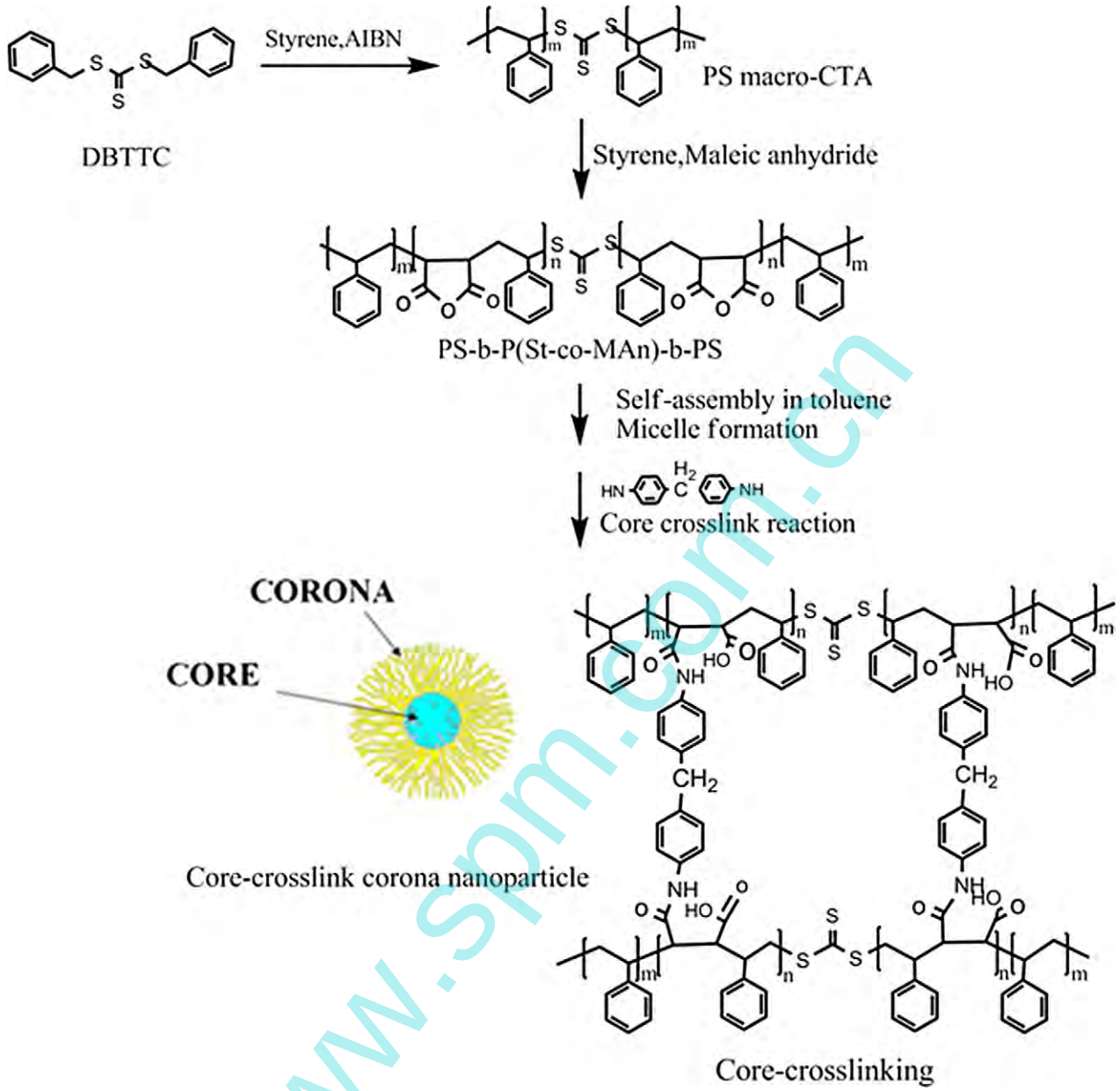

Scheme 1. Synthesis and crosslink reaction of the amphiphilic three-block copolymers PS_m-b-P(St-alt-MAn)$_n$-b-PS_m.

2.6.2. Gel permeation chromatography (GPC)

GPC analysis was carried out with a LC98R1 system equipped with KF-802, KF-803, KF-804 columns and a Shodex R1-71 refractive index detector. THF was used as eluent at a flow rate of 1 ml/min at 35 °C. Mono-dispersed polystyrene standards were used to obtain a calibration curve.

2.6.3. Atom force microscope (AFM)

AFM images were carried out on a scanning probe microscope (CSPM5000, Benyuan Nano Instruments Inc.) in the tapping mode.

2.6.4. Dynamic light scattering (DLS)

The mean particle size (D_h) was determined by DLS. The high performance particle size HPPS 5001 (Malvern) autosizer was used for this purpose. The scattering angle used for the measurement was 90° and the temperature was controlled at 25 °C.

2.6.5. FT-IR

The FT-IR spectra of the copolymer and the core-crosslinked core–corona nanospheres were recorded on a Nicolet Nexus 670 instrument, measured in transmission mode using the KBr self-supported pellet technique.

2.6.6. Optical microscopy observations

Optical microscopy images were obtained in air with a Nicon E600POL Optical microscope.

2.6.7. Scanning electron microscopy(SEM)

Scanning electron microscopy images were recorded using a JEOL JSM-840 apparatus. All of the samples prepared for SEM studies were coated with gold.

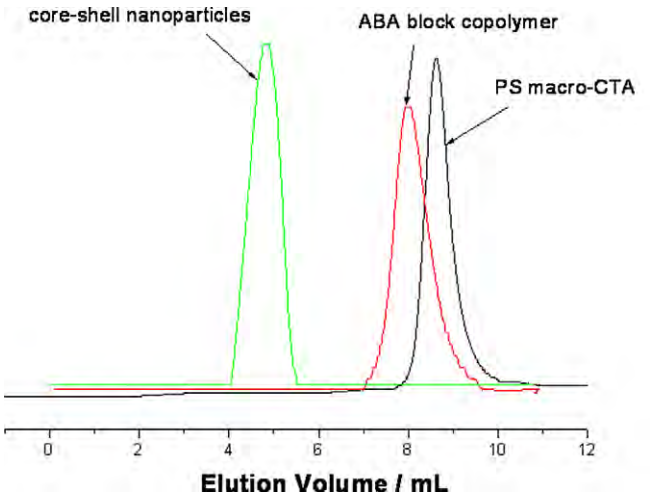

Fig. 1. GPC traces of the PS macro-CTA, ABA type three-block copolymers PS_{100}-b-$P(St\text{-}alt\text{-}MAn)_{98}$-b-$PS_{100}$ and core-crosslinked core–corona nanoparticles.

3. Results and discussion

3.1. Synthesis of PS-b-P(St-alt-MAn)-b-PS

In order to obtain the core-crosslinked core–corona nanoparticles, it is necessary to prepare an amphiphilic block copolymer with a crosslinkable block. The three block copolymer is superior to two block polymer because the two symmetric side block of the three block copolymer can form a more compact corona. The copolymer of maleic anhydride and styrene is used as the middle block not only for its hydrophilic and crosslinkable properties but also for its carboxylic group which can be further incorporated with the growth factor agent as described above. As the maleic anhydride cannot polymerize itself, it is copolymerized with styrene as the middle block. PS is chosen to be the corona for its rigid molecular property which is of vital importance to prepare the honeycomb membrane by emulsion template method.

The synthesis of PS-b-P(St-alt-MAn)-b-PS can be schemed as the above procedure (Scheme 1). The first block PS was polymerized under the chain transfer agent (CTA) DBTTC. The resulted PS homopolymer was used as the macro-RAFT agent to initiate the formation of the middle block containing the copolymer of maleic anhydride and PS. Fig. 1 presents GPC traces of the starting PS macro-CTA and the second-growth three block copolymer obtained by the polymerization. A shift in the GPC trace of the ABA block copolymer compared with the PS homopolymer toward higher molecular weight regions (from $M_n = 21081$ to $M_n = 35671$), with the polydispersity remaining of $M_w/M_n < 1.25$, clearly demonstrates the efficient block formation.

3.2. Core-crosslinked self-assembly

The self-assembly process follows a typical micelle formation process by amphiphilic block copolymer. The polymer PS-P(St-co-MAn)-PS was first dissolved into the THF to form a clear solution. The hydrophobic solvent toluene was then dipped into the solution. The hydrodynamic diameter D_h of the polymer solution was monitored by DLS when varying the toluene concentration (see Fig. 2). At the beginning of the dipping process, the D_h value is close to 0 nm and there are no significant change of the D_h value, which indicates that the copolymer is fully dissolved into the solvent THF. With the addition of toluene, the hydrophobic property of the solvent tends to enhance and the solubility of the hydrophilic PS-co-MAn block gradually declined while the hydrophobic PS block become more soluble. The amphiphilic copolymer began to self-assemble to be core–corona nanoparticles with the hydrophilic PS-co-MAn block as the core and the hydrophobic PS block as the corona. When the toluene concentration reached about 0.02–0.03 wt%, the D_h value abruptly increased to 11.8 nm indicating that the self-assembled nanoparticles were formed and the cmc (critical micelle concentration) was reached. The cmc value is a measurement of the ability of the amphiphilic copolymer to form micelle and it is closely related to the proportion of the two blocks. As shown in Fig. 2 and Table 1 the cmc value decreases from 0.027 to 0.019% by increasing the middle block molar weight from 11,000 to 12,145 indicating that the cmc value tends to fall by increasing the molar weight of the hydrophilic block. No significant change is observed by continuously increasing the toluene amount. The micelle diameter is mono-dispersive as shown in Fig. 3b.

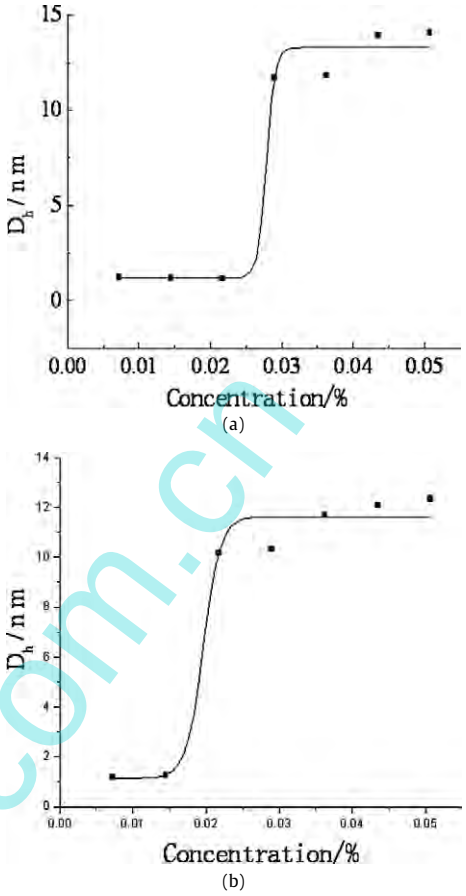

Fig. 2. Concentration dependence of the average hydrodynamic diameter, D_h, of nanoparticles prepared from (a) PS_{50}-$P(St\text{-}co\text{-}MAn)_{45}$-$PS_{50}$; (b) PS_{50}-$P(St\text{-}co\text{-}MAn)_{63}$-$PS_{50}$.

Table 1
Comparison of the cmc value of PS-b-P(St-co-MAn)-b-PS three block copolymer with different middle block molar weight.

Sample	Middle block molar weight	cmc (%)	D_h (nm)
PS_{50}-$P(St\text{-}co\text{-}MAn)_{45}$-$PS_{50}$	11,000	0.027	11.88
PS_{50}-$P(St\text{-}co\text{-}MAn)_{63}$-$PS_{50}$	12,145	0.019	11.36

The formed core–corona nanoparticles were further crosslinked through the reaction of amino diphenyl methane with anhydride in chains at room temperature. Fig. 4 shows the FT-IR of the PS_{100}-b-$P(St\text{-}Alt\text{-}AMn)_{72}$-b-$PS_{100}$ nanospheres before and after reacting with amino diphenyl methane. The band at 1780 cm^{-1} is the anhydride stretching vibrational absorption peak and the band at 1690 cm^{-1} is attributed to stretching vibration of carbonyl group in carboxylic acid group, indicating the generation

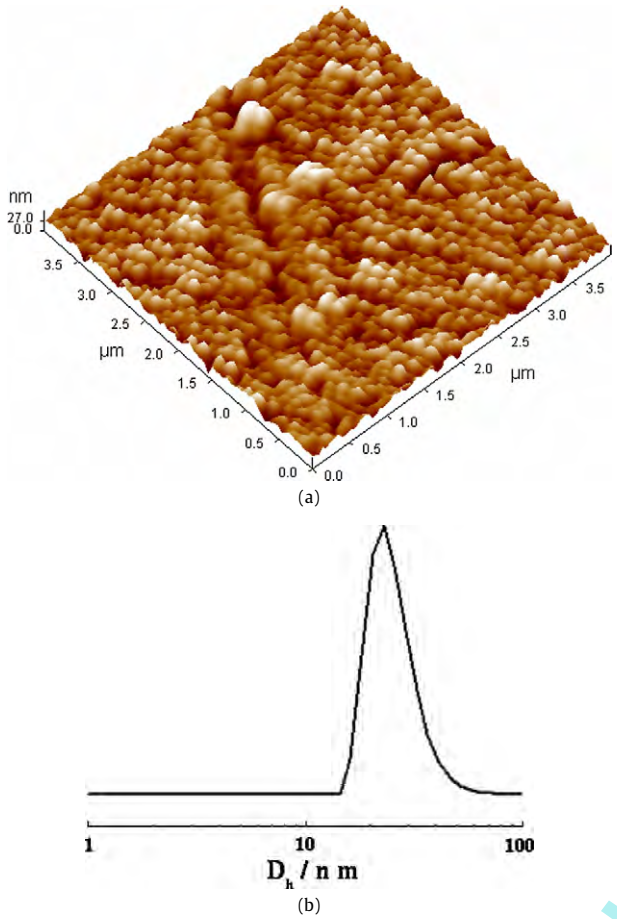

Fig. 3. (a) AFM image of crosslinked core-crosslinked core–corona nanoparticles formed by the self-assembled ABA amphiphilic block copolymer PS_{100}-b-P(St-alt-MAn)$_{98}$-b-PS_{100}; (b) hydrodynamic radius distributions of the core–corona nanoparticles determined by dynamic light scattering (DLS) measurement.

of amic acid. GPC data further confirmed the success of the core crosslink reaction (see Fig. 1), the M_h of the crosslinked nanoparticles is 1,338,500, much larger than the $M_h = 35671$ before the crosslink reaction. The core-crosslinked core–corona nanospheres were then dip-coated onto the glass slides. AFM was used to characterize the morphology of the formed film. As shown in Fig. 3a, the core–corona nanoparticles self-assembled to form a close-packed patterning through the capillary forces. The size of the

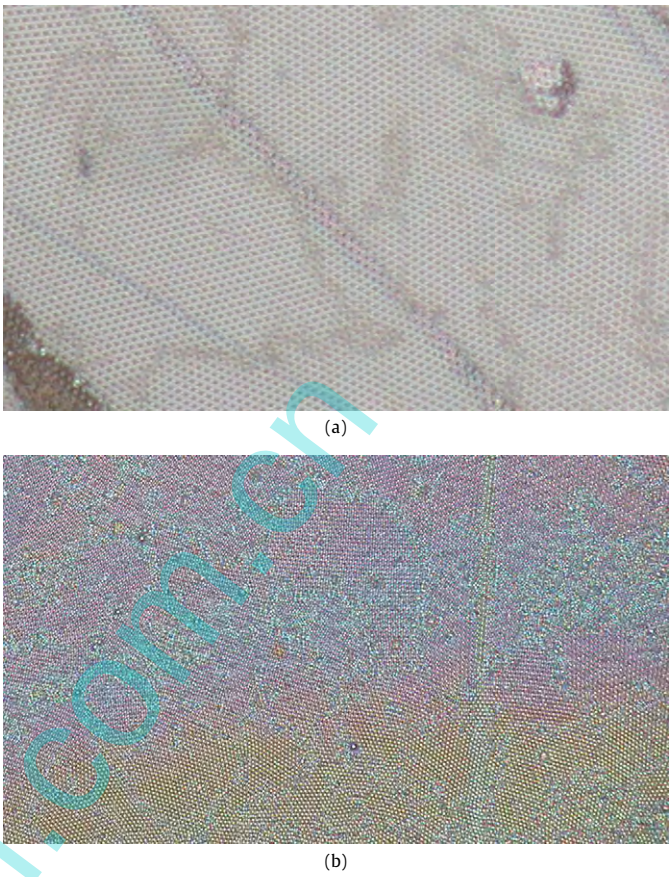

Fig. 5. Optical microscopy image of honeycomb scaffold made from core-crosslinked PS_{100}-b-P(St-co-MAn)$_{26}$-b-PS_{100} core–corona nanoparticles. (a) Scanning mode; (b) transmission mode.

core–corona nanoparticles is mono-dispersed without any large aggregation domain formed (see Fig. 3b).

3.3. Formation of honeycomb film

The honeycomb scaffold microporous films were prepared by casting a 0.5 wt% core–corona nanoparticles solution in carbon disulfide at room temperature under a moist air flow on a substrates such as glass slides. Fig. 5 shows the optical microscopy image of microporous films made from core-crosslinked core–corona

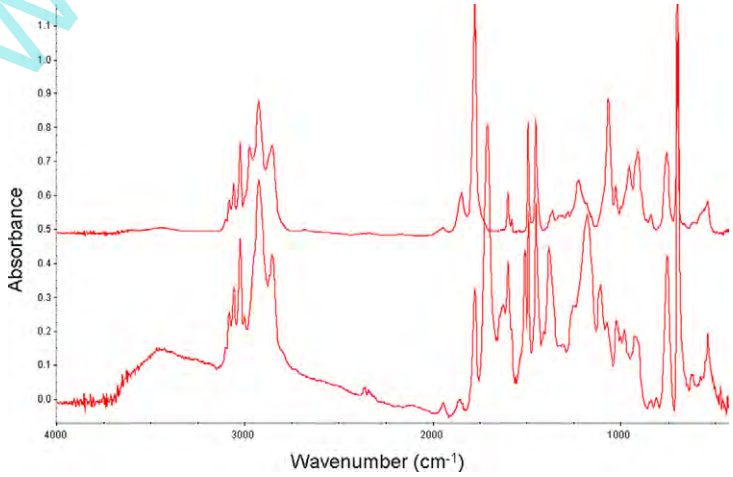

Fig. 4. FTIR spectra of PS_{100}-b-P(St-alt-MAn)$_{98}$-b-PS_{100} three block copolymer before (top spectra) and after (bottom spectra) core-crosslink reaction.

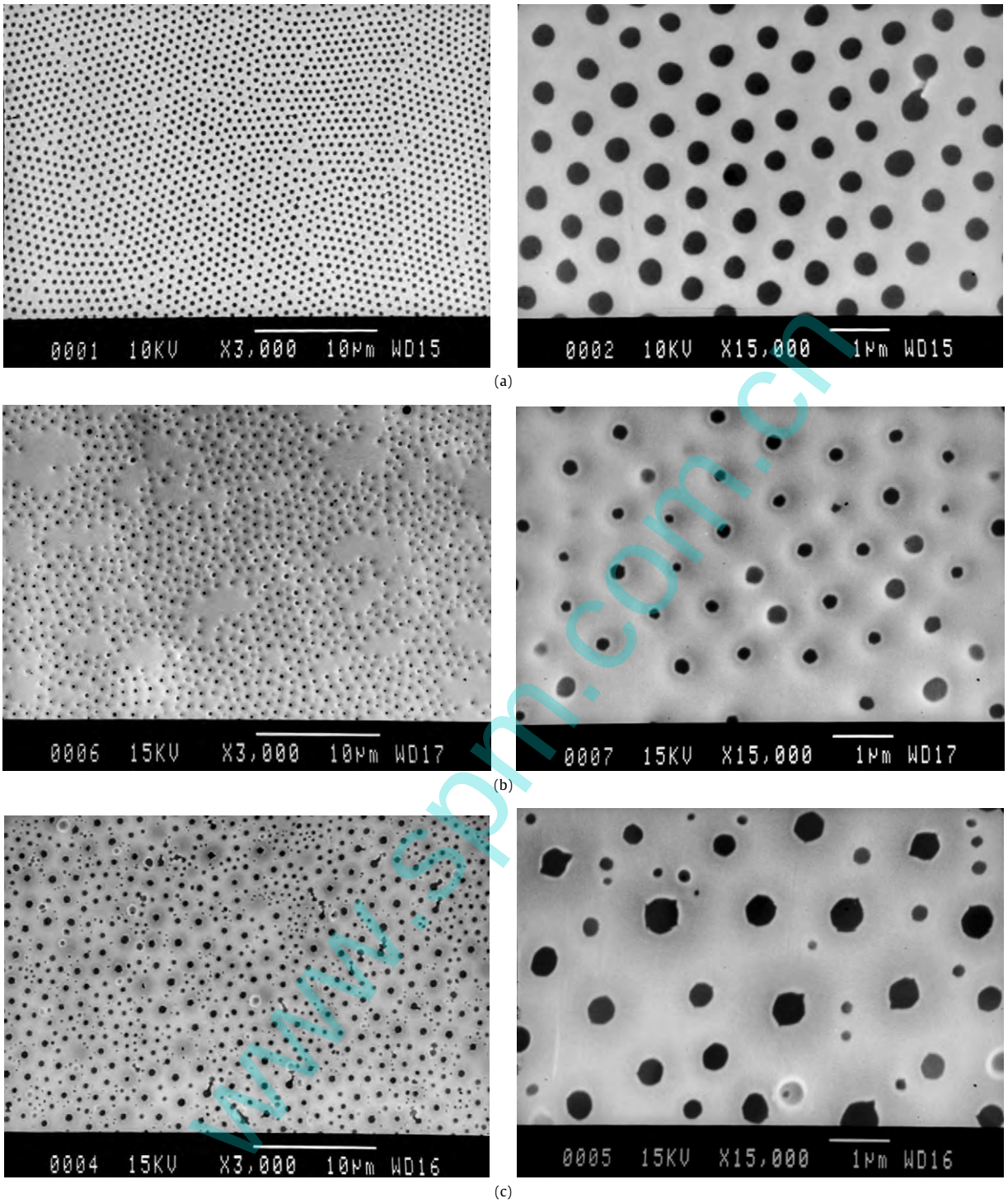

Fig. 6. SEM image of honeycomb scaffold by core-crosslinked core–corona nanoparticles (a) PS_{100}-b-P(St-co-MAn)$_{98}$-b-PS_{100}; (b) PS_{100}-b-P(St-co-MAn)$_{34}$-b-PS_{100}; (c) PS_{100}-b-P(St-co-MAn)$_{26}$-b-PS_{100} (1) magnified by 3000; (2) magnified by 15,000.

nanospheres of PS_{100}-b-P(St-co-MAn)$_{26}$-b-PS_{100}. Such films display bright iridescent colors when viewed from different angles, indicates a periodic refractive index variation, namely photonic band gap crystals [8]. The high degree of order can be assessed from the optical image. The formation of hexagonally packed micropores was clearly observed in the SEM images of the films in Fig. 6a. The honeycomb-formation mechanism involves a combination of complicated thermodynamics and convection phenomenon [22]. When polymer nanoparticles solution are cast from a highly volatile solvent, carbon disulfide, the solvent quickly vaporizes, resulting in rapid cooling of the solution surface owing to the latent heat of evaporation of the solvent, thus initiating the nucleation and growth of moisture, condensation into droplets in the solution. The moist air flow across the surface, coupled with convection currents on the solution surface due to evaporation, force the water droplets to form into a hexagonal close-packing arrays [23,24]. The polymer precipitates from solution at the interface towards these assembled water droplets, creating a solid polymer layer which ultimately encapsulates the isolated water droplets and forms an inverse emulsion on the solution surface [17]. However, very little is known about the role of polymers during the process. Apparently precipitation of the polymer on the interface is the key step to the forma-

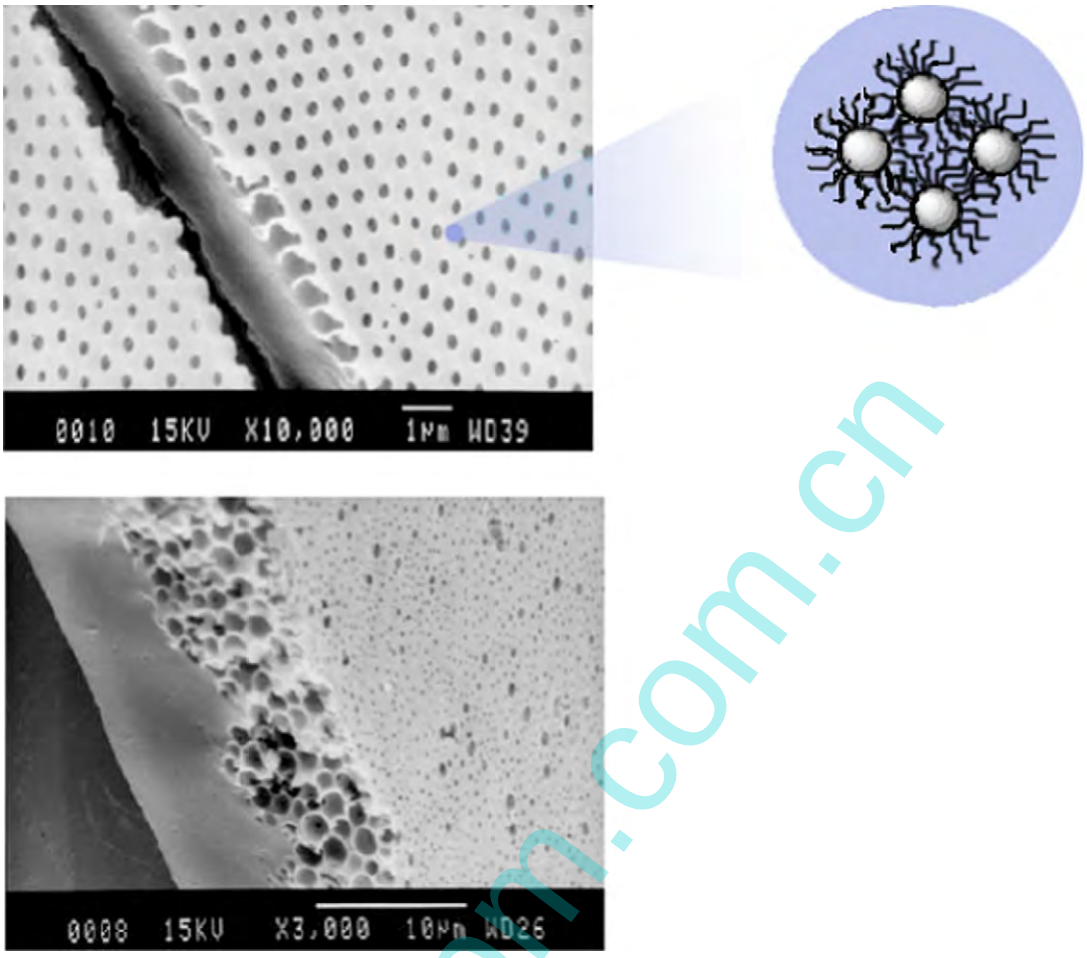

Fig. 7. SEM cross-section image of honeycomb scaffold by PS_{100}-b-P(St-co-MAn)$_{26}$-b-PS_{100} (top image) and PS_{100}-b-P(St-co-MAn)$_{34}$-b-PS_{100} (bottom image).

tion of highly regular honeycomb structures. Many research works confirmed that the regularity of the pore distribution and size of pore is highly related to the molecular properties of the external phase, especially the hydrophilic and hydrophobic ratio of the used block copolymer [25–28]. In this work, since the core and corona of the nanoparticles have different polar, the core corona ratio must be the determinative factor of the pore regularity. To confirm this assumption, three kinds of block copolymers with different hydrophilic and hydrophobic ratios were synthesized and used to prepare the core–corona nanoparticles, namely PS_{100}-b-P(St-co-MAn)$_{26}$-b-PS_{100}, PS_{100}-b-P(St-co-MAn)$_{34}$-b-PS_{100} and PS_{100}-b-P(St-co-MAn)$_{72}$-b-PS_{100}. The SEM images of the films were shown in Fig. 6. The regularity decreases with the increase of the hydrophilic core content. Since the hydrophilic cores of the nanoparticles have good solubility in water, the core blocks tend to point to water droplets to form the inverse emulsion. Like in the case of block copolymer [26], there are two possible mechanisms for the formation of inverse emulsion during the casting process of the nanoparticles, that is, the core block of the nanoparticles may either be swollen and arrange around the water droplets on solution surface or they may rearrange towards the water droplets and solubilize water to form an inverse emulsion within the solution. The monolayer honeycomb porous scaffold tends to follow the first mechanism when the nanoparticles have smaller core corona ratio. The reason is that the porous matrix may precipitate faster with a larger amount of hydrophobic corona, which may prevent the coalescence of the packed water droplets. After the evaporation of the water, the shape of the close packed honeycomb pattern can be observed (Fig. 6a). Increasing the core corona ratio of the nanoparticles may enhance the interaction between the hydrophilic core and the water droplets. This interaction may retard the precipitation of the hydrophobic corona around the water droplet, and reduce the stabilizing effect of the amphiphilic nanoparticles on water droplets. Hence the smaller water droplets tend to coalescence to be larger ones and then sink into the solution which may induce a decrease of the regularity of pore arrays in the scaffold matrix [29] (Fig. 6b). Larger pores may also form when the core corona ratio is large enough due to the coalescence of the water (Fig. 6c). This can lead to the formation of multilayer with a three-dimensionally array of pores and induce the order-disorder transition of the porous structure. Fig. 7 shows the morphologies of scaffolds formed by the two kinds of mechanisms discussed above. It can be seen that the scaffold prepared from the nanoparticles with smaller cores tends to form the monolayer porous structure (Fig. 7 top view) while a transition to the multilayer porous structure will happen when increasing the hydrophilic core size (Fig. 7 bottom view).

4. Conclusion

In conclusion, we have developed a method to produce porous scaffold with hierarchical controllable pore structures. The porous structure was closely related to the molecular structure of the nanoparticles. The core corona ratio determines the size of the pore and the regularity of the pore array. The scaffold prepared from the nanoparticles with smaller core corona ratio tends to form the monolayer porous structure while a transition to the multilayer porous structure will happen when increasing the hy-

drophilic core size. This method offers a route to produce scaffold with controllable macroscale and microscale hierarchical structure. The self-assembled amphiphilic block copolymer nanoparticles served as the building block of the tissue engineering scaffold. As carboxylic groups are formed in the crosslink step of the core, the growth factor which is a necessary protein used in tissue engineering can be incorporated into nanoparticles building blocks. By controlling the self-assembly behavior of the functionalized nanoparticles building blocks, one can obtain the functional porous scaffold easily. This kind of hierarchical honeycomb structure is an ideal candidate for the tissue engineering and drug delivery applications.

References

[1] Li. Xia, X.P. Wang, H.G. Chen, P. Jiang, X.P. Dong, J.L. Shi, Chem. Mater. 19 (2007) 4322–4326.
[2] R. Lakes, Nature 361 (1993) 511–515.
[3] D.Y. Zhao, P.D. Yang, B.F. Chmelka, G.D. Stucky, Chem. Mater. 11 (1999) 1174–1178.
[4] Y.J. Lee, J.S. Lee, Y.S. Park, K.B. Yoon, Adv. Mater. 13 (2001) 1295–1298.
[5] T. Nishikawa, J. Nishida, R. Ookura, S. Nishimura, S. Wada, T. Karino, M. Simomura, Mater. Sci. Eng. C 10 (1999) 141–146.
[6] T. Nishikawa, J. Nishida, R. Ookura, S. Nishimura, S. Wada, T. Karino, M. Simomura, Mater. Sci. Eng. C 8 (1999) 485–500.
[7] M. Shimomura, T. Koito, N. Maruyama, K. Arai, J. Nishida, L. Gråsjö, O. Karthaus, K. Ijiro, Mol. Cryst. Liq. Cryst. 322 (1998) 305–312.
[8] J.E.G.J. Wijnhoven, W.L. Vos, Science 281 (1998) 802–804.
[9] S.G. Zhang, Nat. Biotechnol. 22 (2004) 151–152.
[10] Y.S. Nam, T.G. Park, J. Biomed. Mater. Res. 47 (1999) 8–17.
[11] B. Stropnik, V. Kaiser, Desalination 145 (2002) 1–10.
[12] H.F. Zhang, I. Hussain, M. Brust, Nat. Mater. 4 (2005) 787–793.
[13] M.M. Demir, I. Yilgor, E. Yilgor, B. Erman, Polymer 43 (2002) 3303–3309.
[14] D. Hutmacher, J. Biomater. Sci. Polym. Ed. 12 (2001) 107–124.
[15] K. Stratford, R. Adhikari, I. Pagonabarraga, J.-C. Desplat, M.E. Cates, Science 309 (2005) 2198–2201.
[16] G. Widawski, M. Rawiso, B. Francois, Nature 369 (1994) 387–389.
[17] C. Rodríguez-Abreu, M. Lazzari, Curr. Opin. Colloid Interface Sci. 13 (2008) 198–205.
[18] N.R. Cameron, D.C. Sherrington, Adv. Polym. Sci. 126 (1996) 163–214.
[19] K.L. Wooley, J. Polym. Sci. Part A Polym. Chem. 38 (2000) 1397–1407.
[20] D. Taton, Y. Gnanou, R. Matmour, S. Angot, S.J. Hou, R. Francis, B. Lepoittevin, D. Moinard, J. Babin, Polym. Int. 55 (2006) 1138–1145.
[21] R.T.A. Mayadunne, E. Rizzardo, J. Chiefari, Macromolecules 33 (2000) 243–245.
[22] M. Srinivasarao, D. Collings, A. Philips, S. Patel, Science 292 (2001) 79–83.
[23] M.H. Stenzel, Aust. J. Chem. 55 (2002) 239.
[24] G. Widawski, M. Rawieso, B. Francüois, Nature 369 (1994) 397.
[25] G.D. Fu, E.T. Kang, K.G. Neoh, Langmuir 21 (2005) 3619–3624.
[26] D. Beattie, K.H. Wong, C. Williams, L.A. Poole-Warren, T.P. Davis, C. Barner-Kowollik, M.H. Stenzel, Biomacromolecules 7 (2006) 1072–1082.
[27] T. Hayakawa, H. Yokoyama, Langmuir 21 (2005) 10288–10291.
[28] S.A. Jenekhe, X.L. Chen, Science 283 (1999) 372–375.
[29] M. Srinivasarao, D. Collings, A. Philips, S. Patel, Science 292 (2001) 79–83.